Published January 29, 2016

Evaluation of the CSM-CROPGRO-Canola Model for Simulating Canola Growth and Yield at West Nipissing in Eastern Canada

Qi Jing, Jiali Shang, Budong Qian,* Gerrit Hoogenboom, Ted Huffman, Jiangui Liu, Bao-Luo Ma, Xiaoyuan Geng, Xianfeng Jiao, John Kovacs, and Dan Walters

ABSTRACT

With increasing demands for renewable energy and dietary vegetable oils, the production of canola has become widespread in recent years. Modeling canola growth and yield is a helpful approach to predict canola responses to various environments, especially under climate change. However, few studies have been performed for predicting growth and yield of canola in Canada. In this study, we evaluated the CSM-CROPGRO-Canola model in Decision Support System for Agrotechnology Transfer v4.6 for simulating spring canola at West Nipissing in Eastern Canada. The model was evaluated using plant and soil data collected from field experiments over three growing seasons (2012–2014). The model could predict the observed crop development and successfully mimic the characteristics of canola regarding light absorption and utilization using combinations of leaves and pods. The accumulations of aboveground biomass were satisfactorily simulated in the life cycle under different nitrogen (N) fertilizer application rates, with a normalized RMSE of 19%. The seed yields were successfully predicted with different N application rates except for an underestimation under zero N application. The underestimation of yield under low N rates was possibly related to the deficiency in the simulated N mineralization that could also be associated with inaccurate input soil data. A better simulation of seed yields under low N application was achieved when the soil organic matter module based on the CENTURY model was used in DSSAT v4.6. The calibrated model simulated soil moisture and inorganic N contents satisfactorily, showing a good performance of the CSM-CROPGRO-Canola model for the study region.

Canola was developed in Canada in the 1970s as an edible cultivar of rapeseed (*Brassica napus* L.) with low glucosinolates and low erucic acid. Currently, canola is grown on eight million ha of agricultural land in Canada, which is 22% of the global canola area. More than half of the harvested canola seeds in Canada are exported, accounting for 46% of the international canola market (FAOSTAT, 2015).

The seed yield of canola has doubled since the 1970s (FAOSTAT, 2015), and, with increasing demands for renewable energy and dietary consumption, production is expected to increase. Environmental factors such as temperature, atmospheric CO_2 concentration, and precipitation have a significant effect on crop development and growth (Howden et al., 2007). Facing climate change associated with enhanced greenhouse effects (IPCC, 2007), Canadian climatic conditions are projected to be warmer, with longer growing seasons and increased annual heat units (Qian et al., 2013). However, these changes may also be accompanied by extreme climatic conditions (Qian et al., 2010). These projected climate changes may force canola producers to change cultivars and other management practices to mitigate the potential negative impact on yields and to benefit from the extended growing season. Evaluating canola's response to climate change and management practices through growth experiments in climate chambers can be extremely expensive if not infeasible. On the other hand, crop growth models simulate crop development and soil processes by integrating environmental factors and crop management practices and are thus powerful tools for assessing crop responses to different climatic conditions and crop management practices.

Compared with cereal crops, only a few crop models have been developed for canola. Canola plants have a special biophysical feature in that their pods gradually take over the function of light absorption and photosynthesis during the late growing season as leaves go into early senescence (Gammelvind et al., 1996). Therefore, the total area of leaves and pods function together after flowering, and the plant area index (PAI) rather than leaf area index (LAI) might be more relevant for calculating light interception in canola simulations. By mimicking

Q. Jing, J. Shang, B. Qian, T. Huffman, J. Liu, B. Ma, and X. Geng, Ottawa Research and Development Centre, Agriculture and Agri-Food Canada, Ottawa, Ontario K1A 0C6, Canada; G. Hoogenboom, AgWeatherNet, Washington State Univ., Prosser, Washington 99350-8694; and X. Jiao, J. Kovacs, and D. Walters, Dep. of Geography, Nipissing Univ., North Bay, Ontario P1B 8L7, Canada. *Corresponding author (budong.qian@canada.ca).

Abbreviations: DSSAT, Decision Support System for Agrotechnology Transfer; LAI, leaf area index; LUE, light use efficiency; nRMSE, normalized root mean squared error; PAI, plant area index; SOM, soil organic matter.

Published in Agron. J. 108:1–10 (2016)
doi:10.2134/agronj2015.0401
Received 21 Aug. 2015
Accepted 27 Nov. 2015

Table 1. Summary of experimental treatments for sowing date and fertilizer N applications and attribute measurements.

			Number of measurements‡								
Experiment	Sowing date	N applications†	Phenology	LAI	PAI	AGB	Yield	Leaf N	Grain N	Soil moisture	Soil inorganic N
		kg ha^{-1}									
I	5 May 2012	0; 50; 100; 150	12	12	44	16	4	8	4	52	2
II	15 May 2013	0; 50; 100; 150	13	12	32	16	4	–	–	36	2
III	15 May 2013	0; 50; 100; 150; 200; 50+50; 50+100; 50+150	–	–	–	21	8	–	–	–	–
IV	30 May 2014	0; 50; 100; 150	–	–	–	12	–	–	–	48	–
V	30 May 2014	0; 50; 100; 150; 200; 50+50; 50+100; 50+150	–	–	–	24	–	–	–	–	–

† 50+50 refers to the fertilizer split as 50 kg ha^{-1} at sowing and 50 kg ha^{-1} as topdressing at the 5–6 leaves stage.
‡ AGB, aboveground biomass; LAI, leaf area index; PAI, plant area index.

these characteristics, some crop models have been modified and adapted for canola simulations, such as CERES-Rape (Gabrielle et al., 1998) and LINTUL-BRASNAP (Habekotté, 1997). The APSIM-Canola model was developed to simulate canola in dryland environments in Australia (Robertson et al., 1999), and the CSM-CROPGRO model (Boote et al., 1998) was adapted in the Decision Support System for Agrotechnology Transfer (DSSAT) to simulate spring canola (Saseendran et al., 2010). A more complete adaptation for winter canola under Mediterranean conditions was conducted by Deligios et al. (2013) and has been integrated into DSSAT Version 4.6 (Hoogenboom et al., 2015). The CSM-CROPGRO-Canola model has been evaluated for irrigated conditions but so far has not been evaluated for rainfed and N stress conditions. Few models have been applied for canola simulation in Canada, even though production of the crop in Canada is very important.

The objective of this study was to evaluate the CSM-CROPGRO-Canola model for simulation of canola growth and yield in Canada with different N treatments under rainfed conditions. The model was evaluated with the observed crop development, LAI, PAI, aboveground biomass, and seed yield measured from field experiments conducted at West Nipissing in Eastern Canada during the 2012 to 2014 growing seasons, along with soil moisture and soil inorganic N content observations.

MATERIALS AND METHODS

Field Experiments

The field experiments were conducted in West Nipissing, Ontario, Canada (46°22′ N, 80°5′ W) from 2012 to 2014 and consisted of five different experimental set-ups. Experiments I, II, and IV included four N treatments on 5000-m^2 plots in 2012, 2013, and 2014, whereas Experiments III and V included eight N treatments on 30-m^2 plots in 2013 and 2014. All experiments were conducted using a random design with three to four replicates. Sowing dates, N treatments, and field measurements for all experiments are shown in Table 1.

All plots were located on the same soil polygon of Azilda sandy loam soil in the Canada Soil Information System (CanSIS), Soil Landscapes of Canada (SLC), version 3.2 (Soil Landscapes of Canada Working Group, 2010). The soil consisted of 14% clay, 67% silt, and 2.1% soil organic matter with pH 6.9 in the top 30 cm. The soil bulk density was 1.3 g cm^{-3}. The soil organic matter was only 0.3% below the top 30-cm soil layer. The soil-available inorganic N (nitrate and ammonium nitrogen) content in the top 30-cm layer was measured as 9.08 μg g^{-1} on 11 Apr. 2012, 5.39 μg g^{-1} on 5 May 2013, and 7.75 μg g^{-1} on 6 May 2014. A liquid fertilizer 6–24–6 (N-P-K) at a rate of 47 L ha^{-1} (equivalent to 4.1 kg N ha^{-1}) was applied at field preparation in all the experiments. The canola cultivar used in the experiments was InVigor 5440, known for its consistently high yield and excellent standability. The canola was sowed at a seeding rate of 5.6 kg seeds ha^{-1} at a depth of 0.6 to 1.2 cm and a row spacing of 0.2 m. The plant density was 53 plants m^{-2} in 2012, 50 plants m^{-2} in 2013, and 62 plants m^{-2} in 2014.

During the canola growing season, aboveground biomass was measured three or four times, and crop development was monitored. The green leaf area index was measured in 2012 and 2013 by destructive methods. The PAI in 2012 and 2013 was measured using digital hemispherical photography with a Nikon D300S camera and a 10.5-mm fisheye lens. Photos were taken downward-looking at a height of 50 cm above the top of the crop canopy when it was short and upward-looking from the soil surface when it was tall. The photos were processed using CanEye software (Weiss and Baret, 2010) to derive the effective and total PAI. Details on PAI measurement can be found in Shang et al. (2015). The seed yields were manually measured at maturity in 2012 and 2013, and no yields were measured in 2014 due to waterlogging during canola ripening. Soil moisture in the top 5-cm layer was measured frequently using a Delta-T ML2 Theta Probe in Experiments I, II, and IV. Soil inorganic N content, including ammonium and nitrate content, was measured in Experiment I on 6 June 2012 and in Experiment II on 18 June 2013.

Weather data, including daily maximum and minimum temperature and total precipitation, were obtained from an Environment Canada weather station located close to the experimental field (i.e., North Bay station), and daily solar radiation was calculated using the methodologies proposed by Allen et al. (1998). It was warmer during the 2012 growing season compared with 2013 and 2014. Conditions were wet in August 2012 and 2014 (Table 2).

Crop Model

The CROPGRO model is a generic crop model with a daily time step that computes canopy photosynthesis at hourly time steps using leaf-level photosynthesis parameters and hedgerow light interception calculations. The CROPGRO model

Table 2. Monthly mean temperatures and accumulated precipitation during canola growing season from May to September for 2012–2014.

Month	Minimum temperature			Maximum temperature			Precipitation		
	2012	2013	2014	2012	2013	2014	2012	2013	2014
	°C						mm		
May	7.7	5.9	5.8	20.0	17.9	18.0	51	102	88
June	12.9	10.1	11.4	23.5	20.4	22.9	90	56	68
July	14.6	12.5	10.9	26.4	24.6	22.5	60	129	85
Aug.	13.7	11.8	11.9	23.2	22.4	22.0	146	96	182
Sept.	8.0	6.1	6.9	17.6	17.8	17.4	102	125	98
May–Sept.	11.4	9.3	9.4	22.2	20.6	20.6	449	508	521

was developed as a generic approach for modeling crops in the sense that it has one common source code, yet it can predict the growth of a number of different crops. The model template provides for species, ecotype, and cultivar traits to be defined in the external read-in files for simulations of specific crops, making it easy to adapt for simulating new crops without making changes to the program code. The CSM-GROPGRO-Canola model comes with two soil organic matter (SOM) modules in DSSAT. The default is the original SOM module based on the CERES model (Godwin and Jones, 1991; Godwin and Singh, 1998) and is denoted as G-SOM in this study. The other one was developed by Gijsman et al. (2002) based on the CENTURY model (Parton et al., 1994) and is denoted as P-SOM hereafter. The transport of N as ammonium and nitrate N in each soil layer is associated with water flux obtained from the soil water module. The soil water module (Ritchie, 1998), used by all crop models in DSSAT, computes daily changes in soil water content by soil layer due to infiltration of rainfall and irrigation, vertical drainage, unsaturated flow, soil evaporation, and root water uptake processes. It has been successfully adapted to simulate more than 10 crops, including legumes, oilseed crops, vegetables, and forages, and has been integrated into the DSSAT package (Hoogenboom et al., 2015; Jones et al., 2003). The CSM-CROPGRO model was adapted to simulate canola by Saseendran et al. (2010) based on the module for fava bean (*Vicia faba* L.). In the adaptation, all the parameters related to N fixation processes were turned off from the CROPGRO model, and no N fixation was applied to canola. Later on, the CSM-CROPGRO model was adapted to simulate canola without N and water stresses under a Mediterranean condition based on the parameters used for soybean (*Glycine max* L. Merr.) (Deligios et al., 2013) and became the CSM-CROPGRO-Canola model in DSSAT v4.6.

Model Evaluation

In this study, the crop parameters for canola from Deligios et al. (2013) were set as default values. The default G-SOM module was used to simulate soil N processes. The maximum soil depth was set as 1 m. The soil inorganic N contents, including soil nitrate and ammonia N measured before sowing, were used to initialize the soil N status. The dates on which soil inorganic N content was measured before sowing were set as the dates for the start of simulation each year. Experiments I and II were used to calibrate the model because the data are fairly complete for model calibration. The measured data in Experiment II were first used to calibrate the model for crop development, LAI, aboveground biomass, and seed yield. The measured crop N content data in Experiment I were used to calibrate crop parameters relevant to the N content of leaves and seeds. Crop parameters related to crop development were calibrated first. The parameters that determine the time between emergence and flower appearance were gradually reduced or increased around the default value to make simulated flowering date match the measured value. The same work was done to the parameters that determine other crop development stages. After the parameters for crop development were calibrated, the parameters that determine the leaf area were calibrated. Similarly, the specific leaf area was tuned around the default values to match the simulated LAI with the observed LAI and PAI in the crop life cycle. Associated with each calibration step, a visual graphic comparison was conducted, and the RMSE between simulated and measured values was calculated. The optimum parameters were often obtained with the lowest RMSE. Thereafter, other parameters were calibrated in the same way for aboveground biomass, seed yield, and leaf N concentration. Values of the calibrated parameters are listed in Table 3. Independent data from Experiments III, IV, and V were used for evaluation of the calibrated model.

A paired *t* test [*P*(*t*)] was applied, and RMSE and its normalized version (nRMSE) between simulated (Y_i) and measured (X_i) values were calculated using Eq. [1] and Eq. [2], where n is the number of observations, and $\bar{X}$ is the average of measured values X_i.

$$\mathrm{RMSE} = \left(\frac{\sum (Y_i - X_i)^2}{n} \right)^{0.5} \quad [1]$$

$$\mathrm{nRMSE} = \frac{100 \times \mathrm{RMSE}}{\bar{X}} \quad [2]$$

Model simulation efficiency (EF), mean error (ME) and its relative value rME, and index of agreement (d) between simulated and measured values were also calculated using Eq. [3] through [6] as used in Beaudoin et al. (2008) and Yang et al. (2014).

$$\mathrm{EF} = 1 - \frac{\sum (Y_i - X_i)^2}{\sum (X_i - \bar{X})^2} \quad [3]$$

$$d = 1 - \frac{\sum (Y_i - X_i)^2}{\sum (|Y_i - \bar{X}| + |X_i - \bar{X}|)^2} \quad [4]$$

Table 3. The calibrated tissue composition, genetic coefficients, and photosynthesis parameters in CROPGRO for rapeseed with their default values and calibrated values for canola cultivar InVigor 5440.

Parameter	Definition	Default†	Calibrated
PROLFG	leaf protein content (g g^{-1})	0.210	0.243
PCARLF	leaf carbohydrate content (g g^{-1})	0.620	0.500
PCARST	stem carbohydrate content (g g^{-1})	0.640	0.590
XSLATM	critical temperatures of temperature stress curve on specific leaf area of new leaves (°C)	0, 6, 15, 60	0, 6, 17, 60
FNPGT	daily canopy assimilation in response to average daytime temperature	0, 17, 25, 40	0, 17, 25, 40
XLMAXT	relative rate of photosynthetic electron-transport in response to temperature	0, 25, 28, 35	0, 25, 28, 35
FNPGL	relative effect of minimum night temperature on next day's single-leaf light-saturated photosynthesis rate	−3, 8, 50, 60	−3, 8, 50, 60
PP-SEN	slope of the relative response of development vs. photoperiod (1/h)	−0.0021	−0.011
EM-FL	time between emergence and flower appearance (PD‡)	35	28.5
FL-SH	time between first flower and beginning pod (PD)	9	13
FL-SD	time between first flower and beginning seed (PD)	25	19
SD-PM	time between beginning seed and physiological maturity (PD)	33.6	26.5
FL-LF	time between beginning seed and end of leaf expansion (PD)	3	3
LFMAX	maximum leaf photosynthetic rate (mg CO_2 m^{-2} s^{-1})	1.0	1.28
SLAVR	specific leaf area of cultivar under standard growth conditions (cm^2 g^{-1})	225	330
SIZLF	maximum size of full leaf (cm^2)	95	100
SFDUR	seed filling duration for pod cohort under standard conditions (PD)	23	20
PODDUR	duration of pod addition under standard conditions (PD)	7.5	10
XFRT	maximum fraction of daily growth that is partitioned to seed-shell	1	1
WTPSD	maximum weight per seed (g)	0.0034	0.0034
SDPDV	seeds per pod at standard growth conditions (no. pod^{-1})	22	22
THRSH	threshing percentage [seed (seed + shell)$^{-1}$]	81	81
SDPRO	fraction protein in seeds (g g^{-1})	0.23	0.23
SDLIP	fraction oil in seeds (g g^{-1})	0.48	0.48

† The values for canola were from Deligios et al. (2013).

‡ Photothermal day.

$$\mathrm{ME} = \frac{1}{n}\sum_{i=1}^{n}\left(Y_i - X_i\right) \quad [5]$$

$$\mathrm{rME} = \left(\frac{\mathrm{ME}}{\bar{X}}\right)\times 100 \quad [6]$$

An optimal model reproduces experimental data with $P(t) > 0.05$; RMSE and nRMSE are small, EF and d are close to 1.0, and ME is close to 0.

The P-SOM module was used to verify crop model performance with different SOM modules. All the input parameters from the above calibrations were maintained, except that the G-SOM module was replaced with the P-SOM module. The simulated seed yields for Experiments I, II, and III were compared with the measured values.

RESULTS AND DISCUSSION

Crop Development

The temperature contrast between 2012 and 2013 (Table 2) provided a good opportunity to examine the temperature effects on crop development. The warmer year (2012) showed a 4-d shorter canola growing duration from sowing to maturity than the cooler year (2013). Using the default values of parameters, the simulated flowering dates were much later than the measured ones in all 3 yr. The relevant parameters controlling the lengths of vegetative and reproductive phases were gradually reduced (Table 3) and tuned to match the simulated dates of flowering and maturity with the observed dates in Experiment II. Thereafter, the calibrated model was used to predict the flowering and maturity dates in Experiment I, and the predicted maturity date matched the observed date. The predicted flowering date was only 1 d earlier than the observed date. Therefore, both vegetative and reproductive stages were satisfactorily simulated. This 1-d difference in crop development simulation in this study was better than the model performance in previous studies in which the deviation between the simulated and the measured dates could be as large as 5 d for flowering and maturity (Deligios et al., 2013; Saseendran et al., 2010).

Leaf Area Index and Plant Area Index

The difference in air temperature between 2012 and 2013 (Table 2) was used to improve the calibration of the crop growth parameters related to temperature. One of the critical temperatures controlling specific leaf area (XSLATM) was increased from 15 to 17°C, and the parameter of specific leaf area (SLAVR) was increased from 225 to 330 cm^2 g^{-1} (Table 3). These increased values were based on a comparison between simulated LAI and measured LAI together with PAI from the experiments in 2012 and 2013. The measured LAI and PAI were

similar during the leaf expansion phase in both years; however, the measured PAI values were obviously greater than the measured LAI after peak leaf area stages (Fig. 1). For the treatments with fertilizer N application rates at 50, 100, and 150 kg ha^{-1}, the simulated values were close to the measured values for both LAI and PAI during the increasing phase until the peak stage, but the simulated LAI was greater than the measured values of LAI after the peak. For example, the measured value of LAI was much lower than the simulated LAI on Day 75 after sowing. However, it was interesting to see that the simulated LAIs were similar to the measured PAI throughout the entire growing season. It appeared that the simulated LAI followed the pattern of measured PAI rather than the measured LAI. We believe that this can be explained by the special biophysical feature of the canola crop that green pods take over from fading green leaves for photosynthesis before crop maturity (Gammelvind et al., 1996). In the current version of the CSM-CROPGRO-Canola model in DSSAT v4.6, the functions for light interception and photosynthesis of pods have not been specified, although an individual CROPGRO model has been developed to separately simulate the leaf area and pod area for soybean (Timsina et al., 2007). Alternatively, overestimations of LAI by calibrating LAI with measured PAI data in the late growing season mimicked the function of pods for light interception and photosynthesis in the late growing phase.

The PAI and the LAI for calculating light interception and photosynthesis are specified in some crop models that have been adapted for canola simulation, such as CERES-Rape (Gabrielle et al., 1998), LINTUL-BRASNAP (Habekotté, 1997), and APSIM-Canola (Robertson et al., 1999). In those canola models, the extinction coefficient and radiation use efficiency of pods were generally lower than those of leaves, as has been observed in field experiments (Gammelvind et al., 1996). In the current CSM-CROPGRO-Canola model, pod development and growth were simulated, but the functions for light absorption and use were not specified, although these functions could be implemented in the CROPGRO model.

Biomass and Yield

After the model was calibrated for parameters related to crop development and LAI, crop parameters related to biomass accumulation were calibrated to minimize the gaps between simulated and measured aboveground biomass. Among the parameters, a significant change was made to the maximum leaf photosynthetic rate, which increased from 1.0 to 1.28 mg CO_2 m^{-2} s^{-1} (Table 3). This photosynthetic rate was comparable to the value 1.11 mg CO_2 m^{-2} s^{-1} used in LINTUL-BRASNAP for canola (Habekotté, 1997) and was the intermediate value of measured photosynthetic rates for leaf (1.76 mg CO_2 m^{-2} s^{-1}) and pod (0.66 mg CO_2 m^{-2} s^{-1}) (Gammelvind et al., 1996). The average light use efficiency (LUE) was calculated by the simulated aboveground biomass divided by intercepted photosynthetically active radiation during the whole canola growing season. The average LUE was 2.12 g MJ^{-1} (range, 1.88–2.29 g MJ^{-1}) in this study. The value of LUE in LINTUL-BRASNAP for canola is 2.36 g MJ^{-1} (range, 2.08–2.68 g MJ^{-1}) (Habekotté, 1997). A LUE of 2.4 g MJ^{-1} was used in CERES-Rape (Gabrielle et al., 1998), and a LUE of 2.6 g MJ^{-1} was used in APSIM-Canola

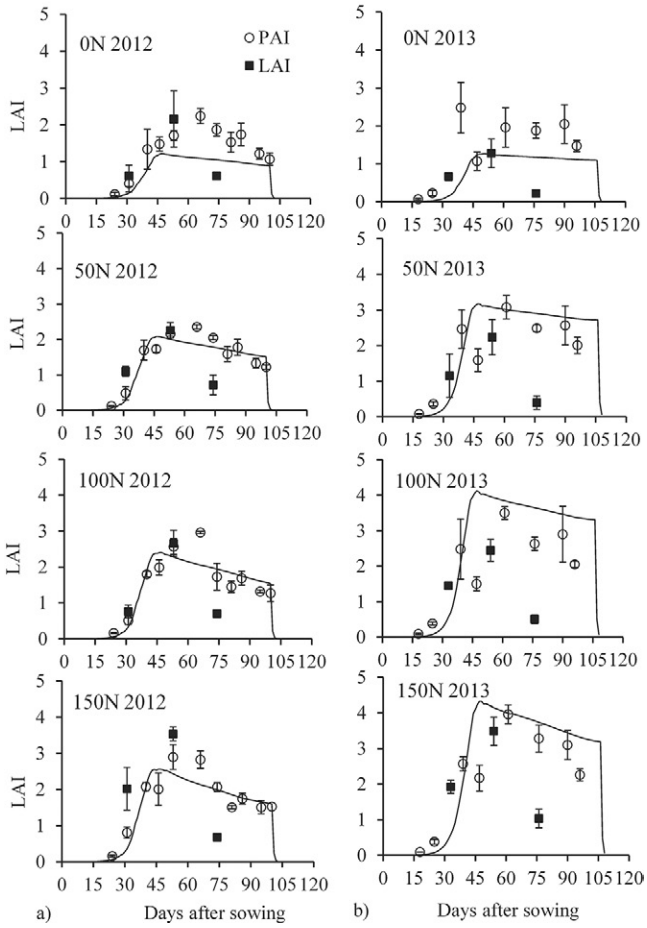

Fig. 1. Simulated leaf area index (LAI) (line) versus measured values (symbols) of plant area index (PAI) (circle) and LAIs (filled square) of Canola under different N fertilizer rates (0N, 0 kg N ha^{-1}; 50N, 50 kg N ha^{-1}; 100N, 100 kg N ha^{-1}; 150N, 150 kg N ha^{-1}) in 2012 (a) and 2013 (b). Whiskers on symbols are the standard deviations of the measurements.

(Robertson et al., 1999). The measured mean value of LUEs was from 1.69 to 3.88 g MJ^{-1} (average, 2.83 g MJ^{-1}) for a spring canola in Western Canada, and the varied LUEs were due to the different plant densities (Morrison and Stewart, 1995). The simulated LUE in this study was within the range of the values in previous studies, indicating that the calibrated value of leaf photosynthetic rate was reasonable for canola grown at West Nipissing in Eastern Canada.

The aboveground biomass was well simulated, with simulated values very close to measured values (Fig. 2). The simulated values were within 1 SD of the measured values at most sampling times for all N treatments (Fig. 2). Model evaluation criteria (Table 4) showed a skillful simulation by the model with respect to the accumulation process of canola biomass. The dynamic simulation on aboveground biomass had a much lower nRMSE in this study (21%) than in the study by Deligios et al. (2013), which reported an nRMSE of 41%. The simulated final aboveground biomass for the evaluation set was compared with measured values (Fig. 3), and pairs of the measured and the simulated biomass were close to the 1:1 line. The final aboveground biomass was simulated very well, with an nRMSE as low as 14% and a small value of rME (1.0%), indicating success in modeling the final aboveground biomass (Table 4).

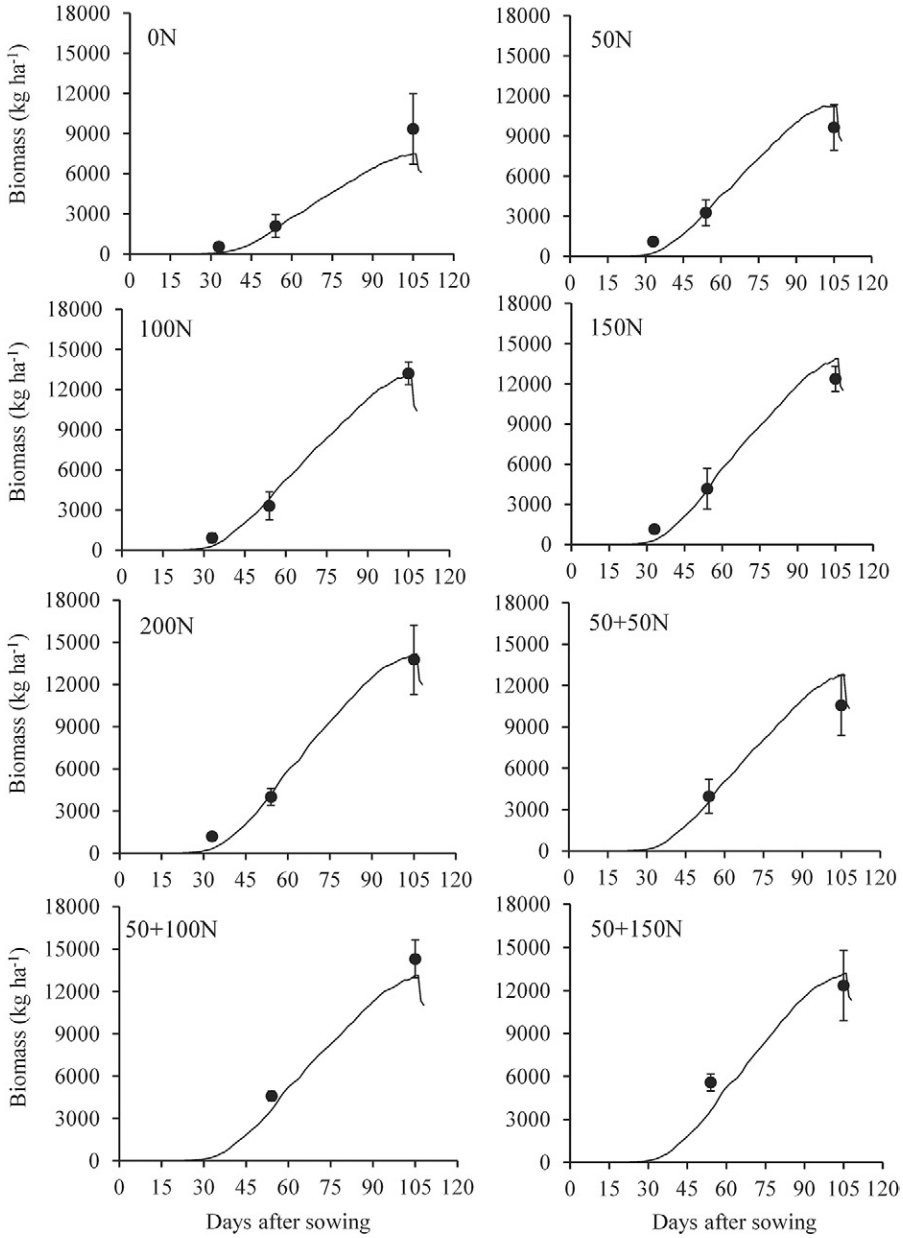

Fig. 2. A comparison between simulated (lines) and observed (symbols) aboveground biomass of canola under different N fertilizer rates (50N, 50 kg N ha^{-1}; 50+50N, 50 kg N ha^{-1} + 50 kg N ha^{-1}) for Experiment III in 2013. Whiskers on symbols are the standard deviations of the measurements.

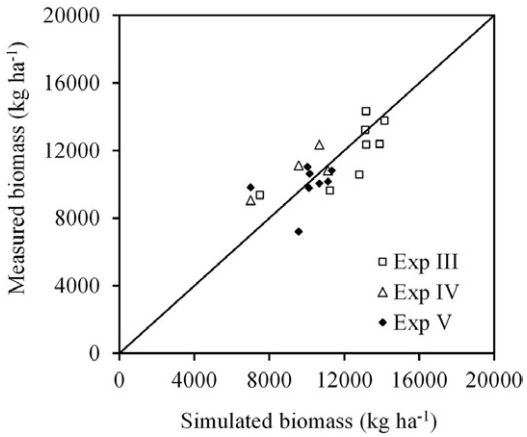

Fig. 3. The 1:1 line to compare simulated with measured aboveground biomass for the evaluation set including Experiments III, IV, and V.

The seed filling duration (SFDUR) was slightly reduced, whereas the duration of pod addition was increased from the default values (Table 3). The seed yields between simulated and measured values for Experiments I and II as calibration data and for Experiment III as an evaluation data set were compared. With various N applications, the simulated seed yield was close to the measured value, mostly within 1 SD, except for the treatment with the very high N rate of 200 kg ha^{-1} (Fig. 4). For the treatments with no N applications, the simulated seed yield was underestimated by more than 1 SD. For the treatments with very high N rates, the simulated yield was higher than the measured yield. Model performance criteria showed that the simulated seed yield was close to the measured values, with $P(t) > 0.05$ and $d > 0.70$. The negative values of EF were mainly associated with the underestimation of seed yields under zero and low N application. The RMSE of the modeled seed yields for the evaluation

Table 4. Statistical criteria for evaluating simulations of aboveground biomass, seed yield, organ N concentrations, soil moisture, and inorganic N content.

Attribute	Statistical criteria†							
	N	*P*(*t*)	RMSE	nRMSE	ME	rME	EF	*d*
				%		%		
			Experiments I and II					
Aboveground biomass, kg ha^{-1}	32	0.18	1676	27	−863	−13.8	0.82	0.96
Final biomass, kg ha^{-1}	8	0.32	1297	12	514	5.0	0.54	0.89
Yield, kg ha^{-1}	8	0.19	576	23	−282	−0.11	−1.5	0.73
Leaf N concentration, %	8	0.36	0.51	14	0.10	0.04	0.55	0.87
Seed N concentration, %	4	0.00	0.36	11	−0.35	−0.11	−18.9	0.74
Soil moisture, cm^3 cm^{-3}	88	0.02	0.06	22	0.03	10.6	0.63	0.88
Soil inorganic N, μg g^{-1}	8	0.41	4	19	1.4	6.1	0.85	0.97
			Experiments III–V‡					
Abovegound biomass, kg ha^{-1}	57	0.27	1165	21	−507	−9.1	0.92	0.98
Final biomass, kg ha^{-1}	20	0.43	1493	14	−104	−1.0	0.21	0.83
Yield, kg ha^{-1}	8	0.32	527	19	181	0.07	−0.44	0.84

† The criteria include the number of measured/simulated data pairs (N), the *p* value from the paired *t* test [*P*(*t*)], RMSE between simulated and measured values with the same unit as corresponding attribute, the normalized RMSE (nRMSE), mean error (ME) with the same unit as corresponding attribute, the relative ME (rME), the model simulation efficiency (EF), and the index of agreement (*d*).

‡ The leaf and seed N concentrations, soil moisture, and inorganic N were not measured in Experiments III, IV, and V, as illustrated in Table 1.

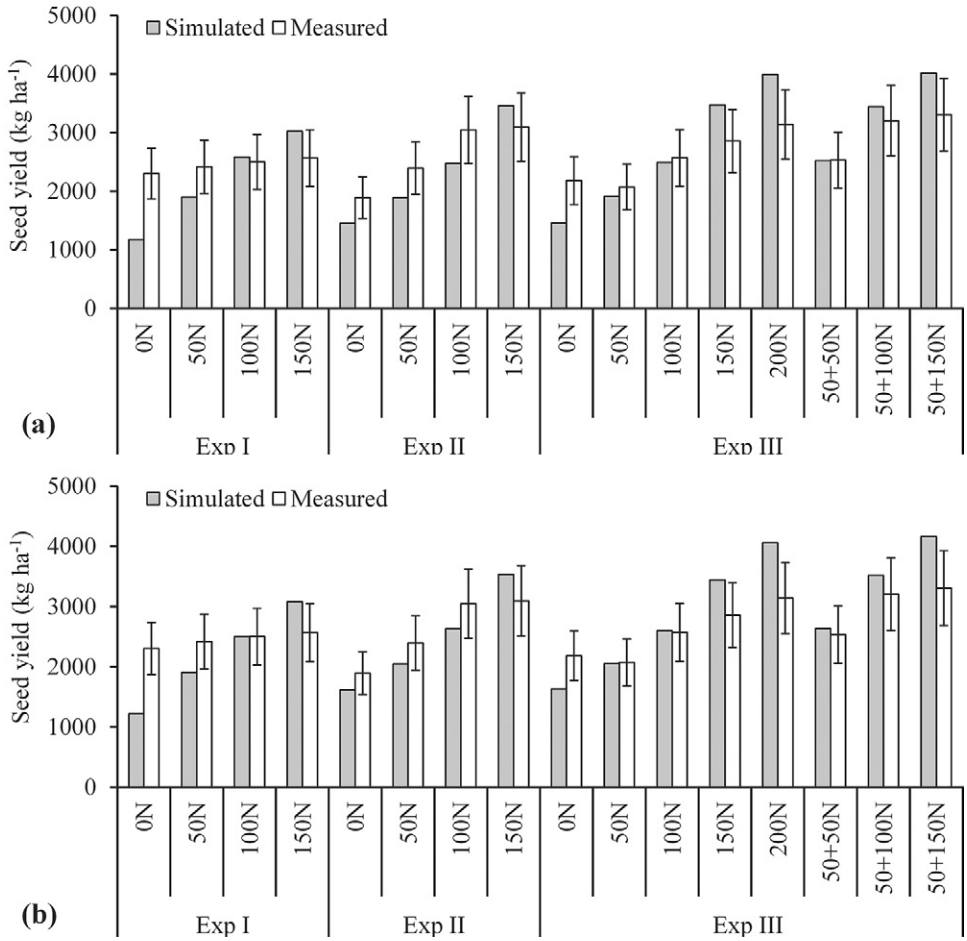

Fig. 4. The measured versus simulated yields of canola in three experiments. The simulated yields were obtained by the CSM-CROPGRO-Canola with (a) the G-SOM module and (b) the P-SOM module. Whiskers on the bars of measured yield are the standard deviations of the measurements.

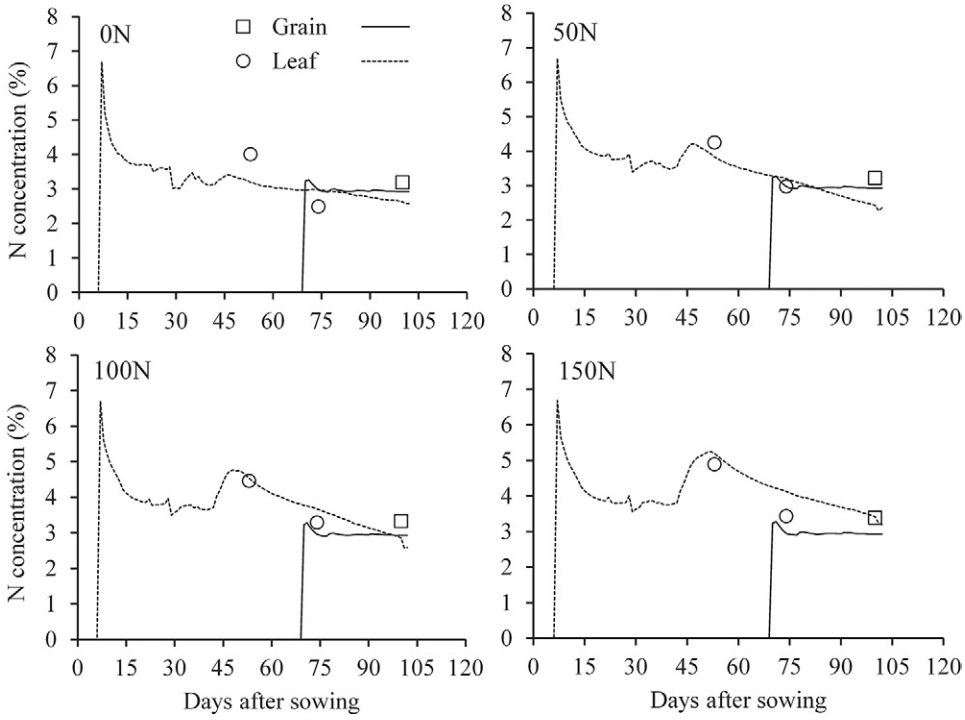

Fig. 5. The comparison between simulated (lines) and measured values (symbols) of N concentrations of canola leaves and grains under different N fertilizer rates (0N, 0 kg N ha^{-1}; 50N, 50 kg N ha^{-1}; 100N, 100 kg N ha^{-1}; 150N, 150 kg N ha^{-1}) in 2012.

data set was 527 kg ha^{-1}, with an nRMSE of 19%. This value of nRMSE for seed yields at maturity was comparable to values (11–34%) obtained by Deligios et al. (2013) in simulating a winter canola in the Mediterranean environment.

The underestimation of seed yields under zero and low N application was likely associated with the simulation of mineralized N with the G-SOM module. The simulated seed yields increased to within 1 SD of measured yields under 0 and 50 kg ha^{-1} in Experiment II when the P-SOM module was used (Fig. 4b). The seed yield was still underestimated under low N application in Experiment I and under no N application in Experiment III, although the simulated yield tended to be closer to the measured yield compared with the values with the G-SOM module. The measured yields with no N applications in Experiment I were close to the yields with 150 kg N ha^{-1}, indicating that the mineralized N amount in the field might be higher than simulated values. The additional mineralized N could come from residues of a previous crop that was not recorded in our experiments. The comparison between the two SOM modules confirmed that the P-SOM module could be more appropriate for use in low-input agricultural systems (Gijsman et al., 2002).

Plant N Concentration

Some parameters associated with organ composition were also calibrated with the measured leaf and grain N concentrations obtained in Experiment I. The leaf protein content (PROLFG) was increased and the carbohydrate contents of leaf and stem were reduced from the default values (Table 3). The simulated leaf N concentration increased with increasing N application rates, consistent with the trend in measured leaf N concentrations with varied N fertilizer applications from 0 to 150 kg N ha^{-1} (Fig. 5). During the growing season, the measured leaf N concentrations decreased from the 50th day after sowing; the simulated values reproduced the decreasing leaf N concentrations, and the simulated values were close to the measured ones (Table 4). The difference in the measured seed N concentrations at harvest under different N treatments was very small, and this was reproduced very well by the model (Fig. 5).

Soil Moisture and Inorganic N Contents

In addition to crop attributes, model performance was also evaluated for soil moisture and inorganic N contents for the different N treatments. Model performance for simulating soil N and moisture can be useful information for a better understanding of the model to improve the simulation accuracy. Soil moisture content in the model responded well to rainfall, as it increased after rainfall events and then decreased due to evapotranspiration by the soil and the crop (Fig. 6). The fluctuations of simulated soil moisture contents matched the patterns of measured soil moisture content, with low values around the 60th day after sowing and high values at the maturity stage. It was apparent that the measured soil moisture content was higher during the period around 60 d after sowing with no N application (>0.2 cm^3 cm^{-3}) than those with various N applications (<0.2 cm^3 cm^{-3}). Soil moisture as a function of different N applications was reproduced by the model. The low moisture content with N applications was likely related to greater transpiration by a larger crop canopy than the case of no N application (Allen et al., 1998). The model performed well, with an nRMSE around 22%. Previous studies also found that the CSM-CROPGRO model could accurately simulate soil moisture contents (Boote et al., 2009; Naab et al., 2004; Sau et al., 2004). Our results were also comparable to those obtained by the STICS model (Beaudoin et al., 2008; Constantin et al., 2012; Jégo et al., 2012). This accurate simulation of soil moisture was the basic requirement for the reliable prediction of soil inorganic N flows (Frolking et al., 1998).

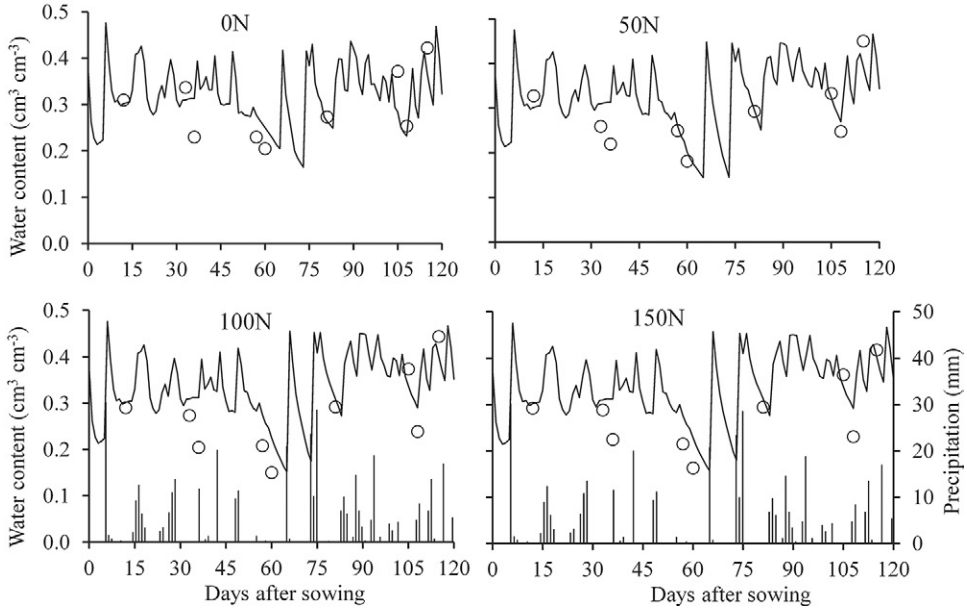

Fig. 6. Simulated soil water content (lines) versus measured values (symbols) for the top 5-cm soil layer during the growing season of canola under different N fertilizer rates (0N, 0 kg N ha^{-1}; 50N, 50 kg N ha^{-1}; 100N, 100 kg N ha^{-1}; 150N, 150 kg N ha^{-1}) in 2013. In the 150N, the bars show daily precipitation.

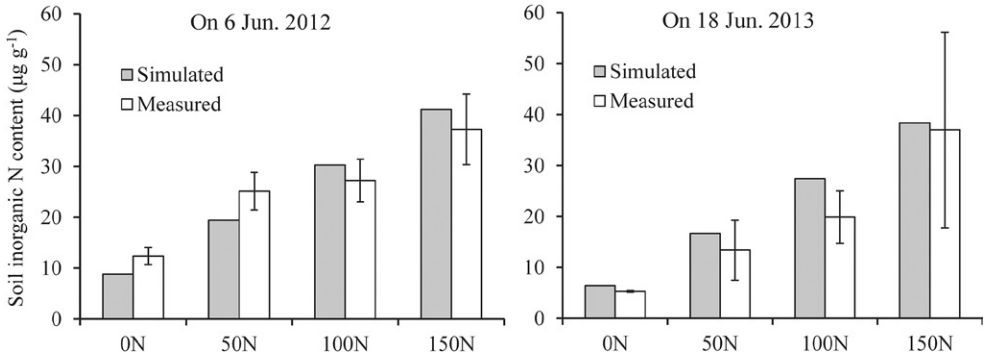

Fig. 7. Simulated soil inorganic N content versus observed values for the top 30-cm soil layer on 6 June 2012 (33 d after sowing) and on 18 June 2013 (35 d after sowing) during canola growing seasons under different N fertilizer rates (0N, 0 kg N ha^{-1}; 50N, 50 kg N ha^{-1}; 100N, 100 kg N ha^{-1}; 150N, 150 kg N ha^{-1}). Whiskers on the bars of the measured are the standard deviations of the measurements.

The simulated soil inorganic N contents matched measured values well. The difference between simulated and measured values was within 1 SD in five out of eight sampling times (Fig. 7). The simulated soil inorganic N contents showed the same pattern as the measured ones (e.g., they tended to increase with increasing N applications at about 1 mo after N application). The performance criteria used in this study (Table 4) indicated a satisfactory simulation regarding soil inorganic N contents. Good simulations for soil moisture and inorganic N content also imply that water and N uptake by the crop were well simulated.

CONCLUSIONS

The CSM-CROPGRO-Canola model was evaluated for spring canola at West Nipissing in Eastern Canada for its performance related to crop development and growth, soil water, and N processes. The calibrated parameters reflected the characteristics of crop development and yield of spring canola. By calibrating modeled LAI against measured PAI, the model was made to accurately predict the crop development in terms of flowering and maturity dates and successfully mimicked the characteristics of canola for light absorption and utilization using combinations of leaf and pods during seed filling. Meanwhile, our calibration did not significantly change the simulations of winter canola grown in the Mediterranean environment that was originally adapted into DSSAT v4.6.

The accumulation of aboveground biomass was well simulated in the life cycle of canola under different N rates. Seed yields were successfully predicted for various N applications but were underestimated with no N applications. Using the P-SOM module improved the simulations on yield under zero and low N applications. The leaf and seed N concentrations were well reproduced by the model under different N application rates.

The model adequately simulated soil moisture contents during the whole canola growing season. Variations of soil inorganic N content under different N treatments were reproduced by the model as well. Satisfactory simulation of soil processes showed a good performance of the CSM-CROPGRO-Canola model for spring canola at West Nipissing in Canada. The evaluated model generally meets the need for applications, such as to simulate the responses of spring canola at West Nipissing to future climate scenarios.

REFERENCES

Allen, R.G., L.S. Pereira, D. Raes, and M. Smith. 1998. Crop evapotranspiration: Guidelines for computing crop water requirements. FAO irrigation and drainage paper 56. FAO, Rome, Italy.

Beaudoin, N., M. Launay, E. Sauboua, G. Ponsardin, and B. Mary. 2008. Evaluation of the soil crop model STICS over 8 years against the "on farm" database of Bruyères catchment. Eur. J. Agron. 29:46–57. doi:10.1016/j.eja.2008.03.001

Boote, K.J., J.W. Jones, G. Hoogenboom, and N.B. Pickering. 1998. The CROPGRO model for grain legumes. In: G. Tsuji, G. Hoogenboom, and P. Thornton, editors, Understanding options for agricultural production. Springer, The Netherlands. p. 99–128.

Boote, K.J., F. Sau, G. Hoogenboom, and J.W. Jones. 2009. Experience with water balance, evapotranspiration, and predictions of water stress effects in the CROPGRO model. In: L. Ahuja, V. Reddy, S. Saseendran, and Q. Yu, editors, Response of crops to limited water: Modeling water stress effects on plant growth processes, volume of advances in agricultural systems modeling. ASA, CSSA, and SSSA, Madison, WI. p. 370–395.

Constantin, J., N. Beaudoin, M. Launay, J. Duval, and B. Mary. 2012. Long-term nitrogen dynamics in various catch crop scenarios: Test and simulations with STICS model in a temperate climate. Agric. Ecosyst. Environ. 147:36–46. doi:10.1016/j.agee.2011.06.006

Deligios, P.A., R. Farci, L. Sulas, G. Hoogenboom, and L. Ledda. 2013. Predicting growth and yield of winter rapeseed in a Mediterranean environment: Model adaptation at a field scale. Field Crops Res. 144:100–112. doi:10.1016/j.fcr.2013.01.017

FAOSTAT. 2015. FAO, Statistics Division. http://faostat3.fao.org/download/T/TP/E (accessed March 2015).

Frolking, S.E., A.R. Mosier, D.S. Ojima, C. Li, W.J. Parton, C.S. Potter, et al. 1998. Comparison of N2O emissions from soils at three temperate agricultural sites: Simulations of year-round measurements by four models. Nutr. Cycling Agroecosyst. 52:77–105. doi:10.1023/A:1009780109748

Gabrielle, B., P. Denoroy, G. Gosse, E. Justes, and M.N. Andersen. 1998. Development and evaluation of a CERES-type model for winter oilseed rape. Field Crops Res. 57:95–111. doi:10.1016/S0378-4290(97)00120-2

Gammelvind, L.H., J.K. Schjoerring, V.O. Mogensen, C.R. Jensen, and J.G.H. Bock. 1996. Photosynthesis in leaves and siliques of winter oilseed rape (*Brassica napus* L.). Plant Soil 186:227–236. doi:10.1007/BF02415518

Gijsman, A.J., G. Hoogenboom, W.J. Parton, and P.C. Kerridge. 2002. Modifying DSSAT crop models for low-input agricultural systems using a soil organic matter–residue module from CENTURY. Agron. J. 94:462–474. doi:10.2134/agronj2002.4620

Godwin, D.C., and C.A. Jones. 1991. Nitrogen dynamics in soil-plant systems. In: J. Hanks and J. T. Ritchie, editors, Modeling plant and soil systems. Agronomy monograph no. 31. ASA, CSSA, and SSSA, Madison, WI. p. 287–321.

Godwin, D.C., and U. Singh. 1998. Nitrogen balance and crop response to nitrogen in upland and lowland cropping systems. In: G.Y. Tsuji, G. Hoogenboom, and P.K. Thornton, editors, Understanding options for agricultural production: System approaches for sustainable agricultural development. Kluwer Academic Publishers, Dordrecht, The Netherlands. p. 55–77.

Habekotté, B. 1997. Options for increasing seed yield of winter oilseed rape (*Brassica napus* L.): A simulation study. Field Crops Res. 54:109–126. doi:10.1016/S0378-4290(97)00041-5

Hoogenboom, G., J.W. Jones, P.W. Wilkens, C.H. Porter, K.J. Boote, L.A. Hunt, et al. 2015. Decision Support System For Agrotechnology Transfer (DSSAT). Version 4.6. www.DSSAT.net. DSSAT Foundation, Prosser, WA.

Howden, S.M., J.-F. Soussana, F.N. Tubiello, N. Chhetri, M. Dunlop, and H. Meinke. 2007. Adapting agriculture to climate change. Proc. Natl. Acad. Sci. USA 104:19691–19696. doi:10.1073/pnas.0701890104

IPCC. 2007. Climate change 2007: The physical science basis. Cambridge Univ. Press, Cambridge, UK.

Jégo, G., J.M. Sánchez-Pérez, and E. Justes. 2012. Predicting soil water and mineral nitrogen contents with the STICS model for estimating nitrate leaching under agricultural fields. Agric. Water Manage. 107:54–65. doi:10.1016/j.agwat.2012.01.007

Jones, J.W., G. Hoogenboom, C.H. Porter, K.J. Boote, W.D. Batchelor, L.A. Hunt, et al. 2003. The DSSAT cropping system model. Eur. J. Agron. 18:235–265. doi:10.1016/S1161-0301(02)00107-7

Morrison, M.J., and D.W. Stewart. 1995. Radiation-use efficiency in summer rape. Agron. J. 87:1139–1142. doi:10.2134/agronj1995.00021962008700060016x

Naab, J.B., P. Singh, K.J. Boote, J.W. Jones, and K.O. Marfo. 2004. Using the CROPGRO-peanut model to quantify yield gaps of peanut in the Guinean Savanna zone of Ghana. Agron. J. 96:1231–1242. doi:10.2134/agronj2004.1231

Parton, W.J., D.S. Ojima, C.V. Cole, and D.S. Schimel. 1994. A general model for soil organic matter dyanmics: Sensitivity to litter chemistry, texture and management. In: R.B. Bryant and R.W. Arnold, editors, Quantitative modeling of soil forming processes. Spec. Publ. 39. SSSA, Madison, WI. p. 147–167.

Qian, B., R. De Jong, S. Gameda, T. Huffman, D. Neilsen, R. Desjardins, et al. 2013. Impact of climate change scenarios on Canadian agroclimatic indices. Can. J. Soil Sci. 93:243–259. doi:10.4141/cjss2012-053

Qian, B., S. Gameda, R. de Jong, P. Falloon, and J. Gornall. 2010. Comparing scenarios of Canadian daily climate extremes derived using a weather generator. Clim. Res. 41:131–149. doi:10.3354/cr00845

Ritchie, J.T. 1998. Soil water balance and plant water stress. In: G. Tsuji, G. Hoogenboom, and P. Thornton, editors, Understanding options for agricultural production. Springer, The Netherlands. p. 41–54.

Robertson, M.J., J.F. Holland, J.A. Kirkegaard, and C.J. Smith. 1999. Simulating growth and development of canola in Australia. 10th International Rapeseed Congress, Canberra, Australia, 26–29 Sept. 1999. CSIRO, Dickson, Australia.

Saseendran, S.A., D.C. Nielsen, L. Ma, and L.R. Ahuja. 2010. Adapting CROPGRO for simulating spring canola growth with both RZWQM2 and DSSAT 4.0. Agron. J. 102:1606–1621. doi:10.2134/agronj2010.0277

Sau, F., K.J. Boote, W.M. Bostick, J.W. Jones, and M.I. Mínguez. 2004. Testing and improving evapotranspiration and soil water balance of the DSSAT crop models. Agron. J. 96:1243–1257. doi:10.2134/agronj2004.1243

Shang, J., J. Liu, B. Ma, T. Zhao, X. Jiao, X. Geng, et al. 2015. Mapping spatial variability of crop growth conditions using RapidEye data in Northern Ontario, Canada. Remote Sens. Environ. 168:113–125. doi:10.1016/j.rse.2015.06.024

Soil Landscapes of Canada Working Group. 2010. Soil landscapes of Canada v3.2. Agriculture and Agri-Food Canada (digital map and database at 1:1 million scale). http://sis.agr.gc.ca/cansis/nsdb/slc/v3.2/index.html (accessed 9 Mar. 2015).

Timsina, J., K.J. Boote, and S. Duffield. 2007. Evaluating the CROPGRO soybean model for predicting impacts of insect defoliation and depodding. Agron. J. 99:148–157. doi:10.2134/agronj2005.0338

Weiss, M., and F. Baret. 2010. CAN-EYE V6.1 user manual. EMMAH, INRA, Avignon, France.

Yang, J.M., J.Y. Yang, S. Liu, and G. Hoogenboom. 2014. An evaluation of the statistical methods for testing the performance of crop models with observed data. Agric. Syst. 127:81–89. doi:10.1016/j.agsy.2014.01.008